Weighted Soft Discernibility Matrix with Deep Learning Assisted Face Mask Detection for Smart City Environment

Imène Issaoui[1,*], Afef Selmi[2]

[1]Unit of Scientific Research, Applied College, Qassim University, Buraydah, Saudi Arabia
[2]Department of Information Technology, College of Computer, Qassim University, Buraydah, Saudi Arabia
Emails: i.issaoui@qu.edu.sa; a.selmi@qu.edu.sa

Abstract

For smart cities to succeed, substantial developments to take place in roads, city streets, public transportation, houses, businesses, and other aspects of city life must be drawn up. In today's world, there is a crucial necessity for effective management of cities to reduce the effect of COVID19 disease with increasing population in cities. Multiple metrics had already been taken to lower the infection rate of COVID19, from the beginning of the outbreaks, such as maintaining distance from another person and wearing face masks. Ensuring security in public places of smart cities needs state-of-the-art technology, including computer vision, deep learning and deep transfer learning for automated detection of face masks and monitoring of whether people wear masks accurately. The achievement of machine learning (ML and) artificial intelligence (AI) techniques in face recognition and object detection makes it fit for the development of FMD methods. The fundamental concept behind the generalized intuitionistic fuzzy soft set is highly productive in making decisions because it considers ways to manipulate an additional intuitionistic fuzzy input from the director to balance any disturbance in the data delivered by the assessment analyst. This manuscript offers the design of Weighted Soft Discernibility Matrix with Deep Learning Assisted Face Mask Detection (WSDMDL-FMD) technique for Smart City Environment. The WSDMDL-FMD technique proficiently discriminates the facial images with the presence or absence of masks. The WSDMDL-FMD technique comprises two stages: Mask RCNN-based face detection and WSDM-based face mask classification. Primarily, the WSDMDL-FMD technique uses Mask RCNN-based face detection. Next, the convolutional neural network (CNN) model derives features from the detected faces and its hyperparameters can be chosen by cuckoo optimization algorithm (COA). For face mask classification, the WSDMDL-FMD technique applies WSDM model. To evaluate the results of the WSDMDL-FMD technique, a series of experiments were involved. The obtained outcomes stated that the WSDMDL-FMD method reaches superior performance than other models

Keywords: Artificial intelligence; Learning System; Smart City; Deep Learning; Face Mask Detection

1. Introduction

Neutrosophic set (N-set) and soft set (S-set) models are the most common theories utilized in uncertainty environments currently, and the NS-set model was developed as a novel hybrid set kind in this area [1]. In this method, soft sets can be employed more practically to state uncertainty issues. The NS set, permitting it to be employed more essentially in uncertainty issues and a comparison among definitions was also prepared [2]. Furthermore, basic set processes have been redefined depending on this definition. Numerous researchers have examined this developed mathematical technique for uncertainty issues [3]. Gradually, infected individuals are quickening vastly because people are not following the compulsory COVID rules like physical distance, keeping rooms well-ventilated, wearing a mask [4], cleaning their hands always, evading crowds, etc [5]. While vaccines have been planned no vaccine is 100 per cent real, it just aids to increase the protection [6]. Surgical Masks, Procedural Face Masks or N95 respirators are few kinds of masks that aid in preventing a diseased individual from spreading the illness to others or stopping a well wearer from the virus [7]. Similarly, mask-wearing decreases the

DOI: https://doi.org/10.54216/IJNS.250116
Received: April 12, 2024 Revised: May 02, 2024 Accepted: June 17, 2024

possibility of other lung disorders like influenza and tuberculosis, arising throughout the epidemic, which might then confuse or worsen the condition [8].

In the present scenario, the area of Computer Vision (CV) is emerging at a fast pace [9]. CV is a sub-division of Artificial Intelligence (AI) that permits computers to remove beneficial data from digital imageries and videos [10]. CV contains numerous sub-domains like Object Recognition, Object Segmentation, and Object Detection, the "Face Mask Detection (FMD) Models" fall below the field named "Object Detection" [11]. Object Detection has dual steps such as Image Classification and Object Localization [12]. Deep learning (DL) development with the combination of CV provides the invention in progress in uncountable areas of technology [13]. Deep neural network (DNN) is the major module of DL methods, which provides object detection, image classification, and segmentation. Convolutional neural network (CNN) is the main method of DNN, which is normally utilized in CV tasks [14]. After training the method, CNN can recognize and classify facial imageries even with slight alterations utilizing their awesome feature extraction skill and keep image pattern facts [15].

This manuscript offers the design of Weighted Soft Discernibility Matrix with Deep Learning Assisted Face Mask Detection (WSDMDL-FMD) technique for Smart City Environment. The WSDMDL-FMD technique proficiently discriminates the facial images with the presence or absence of masks. The WSDMDL-FMD technique comprises two stages: Mask RCNN-based face detection and WSDM-based face mask classification. Primarily, the WSDMDL-FMD technique uses Mask RCNN-based face detection. Next, the convolutional neural network (CNN) model derives features from the detected faces and its hyperparameters can be chosen by cuckoo optimization algorithm (COA). For face mask classification, the WSDMDL-FMD technique applies WSDM model. The obtained outcomes stated that the WSDMDL-FMD method reaches superior performance than other models.

2. Literature Survey

Mostafa et al. [16] present a YOLO-based DL C-Mask technique. After pre-processing, the process of feature extraction is achieved utilizing a CNN method. Furthermore, a Cross-Stage Partial (CSP) DarkNet53 technique is employed to increase the extracting procedure. The data augmentation model is also implemented for feature generation. The feature enhancement task is accomplished by implementing the Spatial Pyramid Pooling Network (SPPNet) and Path Aggregation Network (PANet) approaches. Also, the multi-label classification is utilized for classification. In [17], a FMD technique with IoT is proposed utilizing a fusion DL and "Single Shot Multi-box Detector (SSD)" techniques. The fusion optimization model namely Adaptive Sailfish MFO (ASMFO) is employed for parameter optimization process. Then, Hybrid ResMobileNet (HResMobileNet) model is utilized for classification, in which the parameters are tuned employing a similar ASMFO approach. Moreover, the presented mask detection technique is related to the conventional meta-heuristic models and present classifiers.

Sheikh and Zafar [18] present a framework for the recognition of the face mask that is resilient to adversarial outbreaks. The presented method initially constructed a FMD model by finetuning the MobileNetV2 technique and training it on the adapted dataset. Later, the accomplishment of the method is evaluated by utilizing adversarial images assessed by the fast gradient sign method (FGSM). Lastly, the robustness of the presented method is depicted. AL-Ghamdi et al. [19] propose a novel DL-based FMD in Religious Mass Gathering (DLFMD-RMG) method. The pre-processing process of the DLFMD-RMG model is achieved in two levels namely Contrast Enhancement and Bilateral Filtering (BF). The presented approach employs ResNet-50 along with YOLOv5 techniques for face recognition. Additionally, the accomplishment of the face recognition is enhanced by the seeker optimization algorithm (SOA) approach in order to tune the hyperparameter of the ResNet-50 method. Lastly, the classification of the images is achieved utilizing the Fuzzy Neural Network (FNN) model.

Yasaswi [20] suggests a DL-based model for visual detection of picture processing and parking spaces. Artificial intelligence (AI) models are also utilized. The study also utilized DL models to present a cost-efficient, simple, and dynamic model for recognition. Also, the presented technique implements a Masked Region-Based CNN (MR-CNN) technique and the intersection over union model. Vu et al. [21] proposed an IoT technique depending on a DL model namely YOLO technique. Also, the presented model constructed a mask detection camera (MaskCam) that employs the computing characteristics of NVIDIA's Jetson Nano edge nano devices along with the smart camera application for FMD model. Moreover, a self-built web browsing application is developed with the MaskCam model.

3. The Proposed WSDMDL-FMD Model

In this manuscript, we offer the design of WSDMDL-FMD technique for smart city environment. The WSDMDL-FMD technique proficiently discriminates the facial images with the presence or absence of masks. The

DOI: https://doi.org/10.54216/IJNS.250116
Received: April 12, 2024 Revised: May 02, 2024 Accepted: June 17, 2024

WSDMDL-FMD technique comprises two stages: mask-based face detection and WSDM-based face mask classification as illustrated in Fig. 1.

A. Face Detection Module

Primarily, the WSDMDL-FMD method exploits Mask RCNN-based face detection. CNN known as Mask-RCNN is used in this study [22]. This model expands the Fast-RCNN by integrating another branch to predict the pixel-level segmentation mask for all the detected objects. In this paper, it is suitable for the studied application because it incorporates instance segmentation and object detection tasks. The network structure includes three major elements: a region proposal network (RPN) to suggest the ROI for the object segmentation, a convolutional backbone for feature extraction, and an ROI head and box head to select the region and refine the boundary for more accurate segmentation. In Mask RCNN architecture, hyperparameter setting is most critical factors which influence the behaviours of Mask RCNN during the inference and training phases. This hyperparameter, including number of iterations, learning rate, and batch size, considerably influences performance of the model.

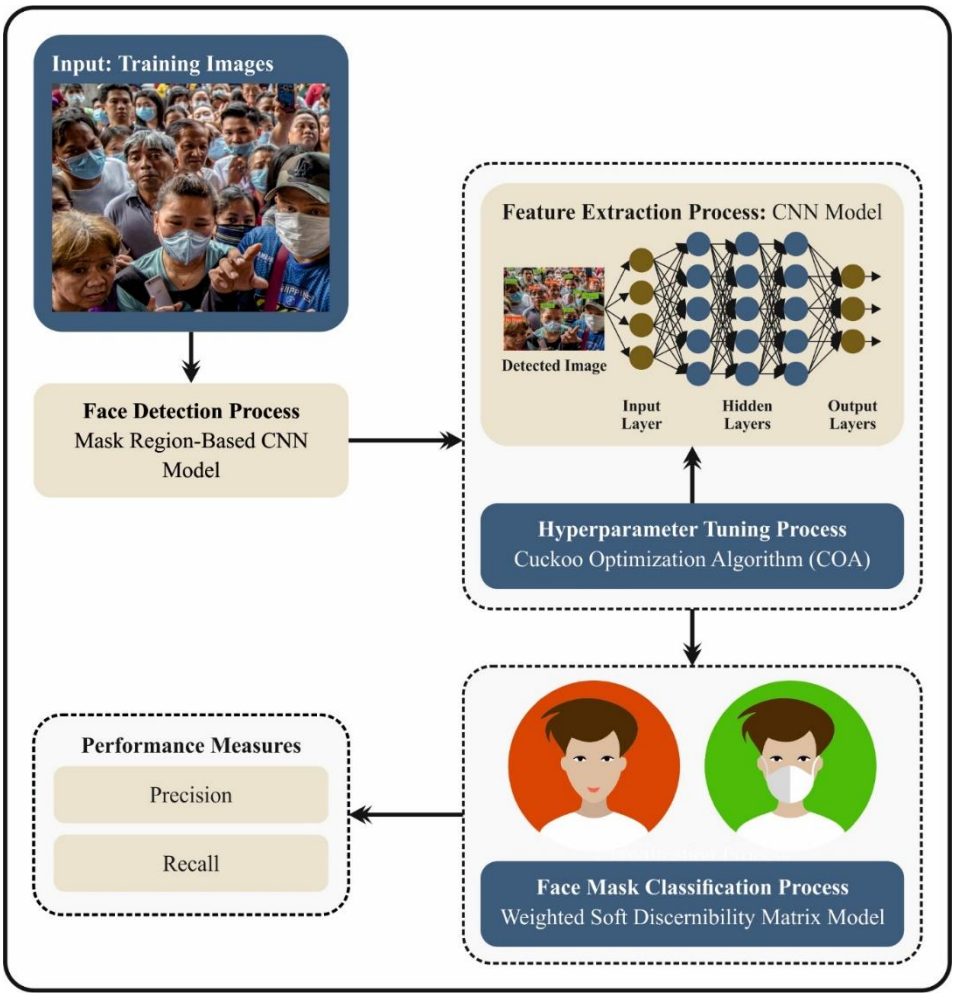

Figure 1: Workflow of WSDMDL-FMD technique

B. Face Mask Classification Module

a) CNN Architecture

Next, the CNN model derives features from the detected faces. A great ML model, CNN are aided type of neural network [23]. CNN uses many mathematical methods such as regularization, backpropagation (BP) and gradient descent. Convolution (Conv), max-pooling, and fully connected (FC) layer are 3 foremost layers of a CNN method. Fig. 2 illustrates the architecture of CNN.

Conv Layer: This layer is a main part of CNN. Filtering is executed in exact settings to offer few outputs from input in this layer. The neurons are organized in a a rectangular grid. So this indicates that the filters can contain a rectangle grid or a cubic block. It is functional from the topmost left to the bottommost right. A novel neuron was

DOI: https://doi.org/10.54216/IJNS.250116
Received: April 12, 2024 Revised: May 02, 2024 Accepted: June 17, 2024

attained after computing the weight size of pixels by $w^t x + b$. The output size is measured by 3 kinds of hyperparameters in this layer such as depth, stride and zero padding.

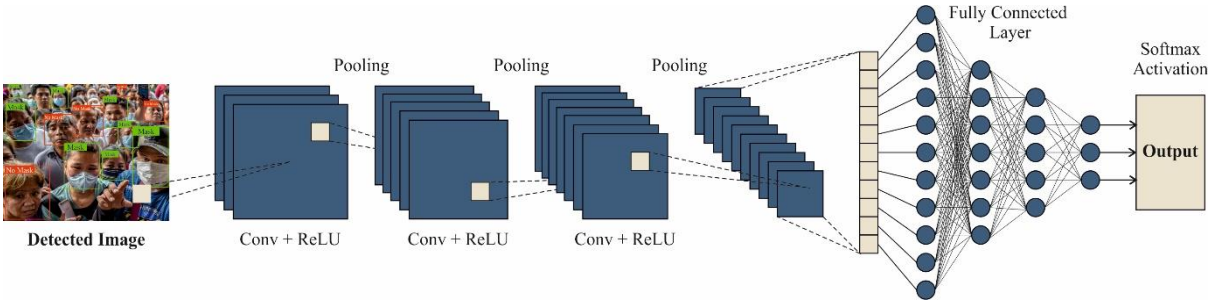

Figure 2: CNN Architecture

The stride identifies filters by pixels in the input neuron. Also, it states that the space or the amount of pixels the filter avoids or changes over in an input pixel matrix. If the stride value is 2 or higher, a huge stride produces a lesser output. Where Zero padding is employed when the filter is not appropriate in an input image. It is nothing but the filling procedure with 0 for regulating the dimension of the input neuron. It is naturally employed if the input dimension in output neuron wants to be preserved. The below-mentioned calculation is employed in order to compute size of output neurons:

$$Output = \frac{w - k_s + 2p_s}{St} + 1 \quad (1)$$

Here, k_s represents the filter size, p_s refers to the padding size, St denotes the stride and w signifies the input neuron size. In addition, linear algebraic processes are used in CNN. Assume that the matrix sizes are X and Y, whereas Y displays the column and X displays the row. A two-dimensional convolutional cube computes the 2D Conv with 2 matrices of input. The size of matrix for M and N are (X_M, Y_M) and (X_N, Y_N), respectively. The Conv formulation is given below if the cube defines the whole size of output.

$$C(a,b) = \sum_{x=0}(X_M - 1)\sum_{y=0}(Y_M - 1)M(x,y) * N(a-x, b-y) \quad (2)$$

Where

$$0 \le a < X_M + X_N - 1 \; and \; 0 \le b < Y_M + Y_N - 1. \quad (3)$$

Max-Pooling Layer: This executes the subsequent process after every Conv layer. The size of input neuron was decreased by utilizing the pooling layer. It models the Conv layer of small rectangular blocks and obtains them to yield only output from every block. The below-mentioned formula is the max −pooling layer:

$$h_j^k = \max_{\overline{a} \in N(a), \overline{b} \in N(b)} h_j^{k-1}(\overline{a}, \overline{b}) \quad (4)$$

This layer is formed by using the filters and sampling them in every layer.

FC Layer: It is formed by linking all previous neurons. Because it was linked from every input to output neuron, this layer normally boosts decreasing spatial data. The BP model is nothing but a gradient descent-based model which centers its FF on declining cross-entropy loss to minimise NN fault

$$P = \sum_{a=1}^{X}\sum_{b=1}^{Y} - s_a^{(b)} \log d_a^{(b)} \quad (5)$$

Here, X denotes the no. of samples, $s_a = (0, \ldots, 0, 1, \ldots, 1, 0, \ldots, 0)$ and d_a are the required output vectors, and the output vector where the subsequent formulation can achieve:

$$d_a^{(b)} = \frac{e^{fa}}{\sum_{a=1}^{Y} e^{fa}}. \quad (6)$$

The weighted penalty is assumed to emerge the L function to comprise a value of η to increase weight value.

DOI: https://doi.org/10.54216/IJNS.250116
Received: April 12, 2024 Revised: May 02, 2024 Accepted: June 17, 2024

$$P = \sum_{a=1}^{X}\sum_{b=1}^{Y} - s_a^{(b)} \log d_a^{(b)} + \frac{1}{2}\varphi \sum_{P}\sum_{Q} e_{p,q}^2 \quad (7)$$

Here, P signifies the total amount of layers, e_p represents the weight of connection, and Q displays layer 1 connection.

b) COA-based Parameter Selection

For parameter selection, the hyperparameters can be chosen by COA. Yang and Deb In 2009, established COA, a nature-inspired metaheuristic algorithm [24]. The obligate brood parasitism includes many different kinds of cuckoos, making it to lay the egg on the nest of other host birds. The female cuckoos are used to imitate the egg and color of other cuckoo species. This boosts their reproductive ability and reduces the relinquishment probability. In the optimization algorithm, there are three idolized rules which explain their application. A metaheuristic approach for the random exploration of the optimum strategy within the search range heavily relies on randomization. Random walking is employed in carrying out this randomization. The randomized walking is presented for the COA by using Lévy fight (LF) to increase the efficiency of search space in unpredictable circumstances. The LF provides a randomized walking based on the distribution of Lévy's power law as demonstrated in Eq. (8),

$$Lévy \sim u = t^{-\lambda}, (1 < \lambda \leq 3) \quad (8)$$

Where u denotes the Lévy distribution. New one surrounds the optimal solution, which accelerates the local search.

The new strategy by using LFs and their fitness is compared with initial cuckoo population n for the nest x_j and the leftover eggs in the nest for the objective function $f(x) = (x_1, \ldots, x_d)^t$. If the updated solution is superior to the randomly chosen nest then it replaces the egg with new egg. While most of the worst nests are ignored, the optimum solution is retained for further analysis. The new solution, $x_i^{(t+1)}$ from LFs, is performed by using Eq. (9):

$$x_i^{(t+1)} = x_i^t + \alpha \oplus Levy(\lambda) \quad (9)$$

The entry-wise multiplication is represented by the product, if $\alpha > 0$ then the stepsize related to the scale is 1.

The fitness selection is the major factor which effects the COA performance. The hyperparameter selection method includes the solution encoding technique for assessing the efficiency of the solution candidate. Here, the COA deliberates accuracy as the most important condition to design the FF.

$$Fitness = \max(P) \quad (10)$$

$$P = \frac{TP}{TP + FP} \quad (11)$$

Where TP and FP are the true and the false positive values.

c) Classifier Selection

For face mask classification, the WSDMDL-FMD technique applies WSDM model. In this part, we provide the main descriptions of fuzzy set (FS), intuitionistic fuzzy set (IFS), soft set (SS), generalized IFSS, soft discernibility matrix (SDM) and weighted soft discernibility matrix (WSDM) [25].

In this research work, finite set $\hat{Y} = \{\ell_1, \ell_2, \ldots, \ell_n\}$ and $\hat{P} = \{e_1, e_2, \ldots, e_m\}$ signifies the group of m attributes and n alternatives. An FS is definite to handle uncertainty depending upon the opinion of gradualness efficiently.

Description 1. The membership value $\xi_A : \hat{Y} \to [0,1]$ describes the FS A over the $\hat{Y}$, while $\xi_A(\ell)$ specified the membership of a group $\ell \in \hat{Y}$ in FS $\hat{A}$.

Similar to membership degree, human perception states that there is a non-membership grade of a group. Moreover, an IFS is definite by Atanassov to outline the vagueness of individuals when need the verdicts over the origins.

Description 2. An IPS $\hat{A}$ over the space $\hat{Y}$ is definite below

DOI: https://doi.org/10.54216/IJNS.250116
Received: April 12, 2024 Revised: May 02, 2024 Accepted: June 17, 2024

$$\hat{A} = \{(\ell, \xi_{\hat{A}}, \vartheta_{\hat{A}}) | \ell \in \hat{Y}\}, \quad (12)$$

Whereas, $\xi_{\hat{A}} : \hat{Y} \to [0,1]$ and $\vartheta_{\hat{A}} : \hat{Y} \to [0,1]$ denotes the grade of positive and negative memberships, correspondingly. Moreover, it is essential that $0 \leq \xi_{\hat{A}} + \vartheta_{\hat{A}} \leq 1$.

A SS delivers an effectual structure to deal with vagueness with the parametric opinion, that is, every group is estimated by few norms of features.

Description 3. Assume that $\hat{p}$ is a parameter space, $\hat{Y}$ is a universe set, $\hat{A} \subseteq \hat{p}$ and $\hat{P}(\hat{Y})$ are the power set of $\hat{Y}$ · A pair $(\hat{\mathcal{F}}, \hat{A})$ is known as an SS over $\hat{Y}$, whereas $\hat{\mathcal{F}}$ is a set-valued map assumed by $\hat{\mathcal{F}} : \hat{A} \to P(\hat{Y})$.

Description 4. Let $\hat{p}$ is a parameter space, $\hat{Y}$ is a universal set, $\hat{A} \subset \hat{p}$ and IF $(\hat{Y})$ the set every IFS of Y. A pair $(\hat{\mathcal{F}}, \hat{A})$ is named an IFSS over Y, while $\hat{\mathcal{F}}$ is a set-valued map known by $\hat{\mathcal{F}} : \hat{A} \to IF(\hat{Y})$.

The GIFSS idea is very inspiring in decision-making because it studies how to exploit a further input of intuitionistic fuzzy to diminish any probable distortion in the data delivered by assessing specialists. Initially, the author explains the GIFSS, but it contains some issues, so, Feng re-defines the GIFSS, which is given below.

Description 5. Assume that Y as a collection of universe, $\hat{A} \subset \hat{p}$ is a set of parametric. By a GIFSS, thus $(\hat{\mathcal{F}}, \hat{A}, \hat{\rho})$, where $(\hat{\mathcal{F}}, \hat{A})$ denotes the IFSS over $\hat{Y}$ and $\hat{\rho} : \hat{A} \to IF(\hat{A})$ denotes an IFS in $\hat{A}$.

Here, $(\hat{\mathcal{F}}, \hat{A})$ is termed basic IFSS (BIFSS) and $\hat{\rho}$ is termed the parametric IFS (PIFS).

In, Q. Feng describes the SDM for SS, which delivers the finest alternative and also an order relation between every alternative.

Description 6. Here $(\hat{\mathcal{F}}, \hat{A})$ be an SS over $\hat{Y} \cdot \hat{\mathcal{F}}$ defined the partition UIND $(\hat{\mathcal{F}}, \hat{A}) = \{N_j : i \leq |\hat{Y}|\}$ of $\hat{Y}$. The SDM is described as $M = (M(N_j, N_j))_{i,j \leq |\hat{Y}|}$, whereas $M(N_i, N_j)$ is named the SDP between N_i and N_j, which is defined below

$$M(N_i, N_j) = \{\hat{E}^i \cup \hat{E}^j : i, j \leq |\hat{Y}|\}. \quad (13)$$

In which

$\hat{E} = \{\epsilon_p^i : \hat{\mathcal{F}}(\ell_i, \epsilon_p) = 1$ and $\hat{\mathcal{F}}(\ell_j, \epsilon_p) = 0, \forall \ell_i \in N_i, \forall \ell_j \in N_j\}$

and

$\hat{E}^j = \{\epsilon_p^j : \hat{\mathcal{F}}(\ell_j, \epsilon_p) = 1$ and $\hat{\mathcal{F}}(\ell_j, \epsilon_p) = 0, \forall \ell_j \in N_j, \forall \ell_j \in N_i\}$.

The symbol ϵ_p^i (or ϵ_p^j) signifies the element in N_j (or N_j), which contains the 1 value at the attribute ϵ_p, i.e., $\hat{\mathcal{F}}(\ell_i, \epsilon_p) = 1, \ell_j \in N_i$ $(or\ \hat{\mathcal{F}}(\ell_j, \epsilon_p) = 1, \ell_j \in N_j)$.

The WSDM is definite below.

Description 7. Where, $(\hat{\mathcal{F}}, \hat{A})$ is an SS over $\hat{Y} \cdot \hat{\mathcal{F}}$ defined the partition UIND $(\hat{\mathcal{F}}, \hat{A}) = \{N_i : i \leq |\hat{Y}|\}$ of $\hat{Y}$. The WSDM is definite as $\mathcal{M} = (M(N_i, N_j))_{i,j \leq |\hat{Y}|}$, whereas $M(N_i, N_j)$ is named the SDP among N_i and N_j and expressed as

$$M(N_i, N_j) = \{\hat{E} \cup \hat{E} : i, j \leq |\hat{Y}|\}. \quad (14)$$

In which

$$\hat{E}^i = \{\epsilon_p^{i*\hat{\omega}_i} : \hat{\mathcal{F}}(\ell_i, e_p) = 1\ and\ \hat{\mathcal{F}}(\ell_j, \epsilon_p = 0, \forall \ell_j \in N_i, \forall \ell_j \in N_j\}$$

and

$\hat{E}^j = \{\epsilon_p^{j*\hat{\omega}_j} : \hat{\mathcal{F}}(\ell_j, e_p) = 1$ and $\hat{\mathcal{F}}(\ell_i, \epsilon_p) = 0, \forall \ell_j \in N_j, \forall \ell_i \in N_i\}$.

The symbol $\epsilon_p^{i*\hat{\omega}_i}$ (or $\epsilon_F^{j*\hat{\omega}_j}$) signifies the elements in N_i (or N_j), which contains the value 1 at the parameter e_p, i.e., $\hat{\mathcal{F}}(\ell_i, \epsilon_p) = 1, \ell_j \in N_i\big(or\ \hat{\mathcal{F}}(\ell_j, \epsilon_p) = 1, \ell_j \in N_j\big)$.

DOI: https://doi.org/10.54216/IJNS.250116
Received: April 12, 2024 Revised: May 02, 2024 Accepted: June 17, 2024

Also, Q. Feng provides few assets of SDM and WSDM.

Proposition 1. Let the $(\hat{\mathcal{F}}, \hat{A})$ be an SS over $\hat{Y}$, whereas $\hat{Y} = \{\ell_1, \ell_2, \ldots, \ell_n\}$ and $\varphi(N_i, N_j) = |M(N_i, N_j)|$. The following are the features of SDM:

1: $M(N_i, N_i) = \emptyset(\forall i \leq n)$;

2: $M(N_i, N_j) = M(N_j, N_i)(\forall i, j \leq n)$;

3: $\varphi(N_i, N_i) = 0(\forall i \leq n)$;

4: $\varphi(N_j, N_j) = \varphi(N_j, N_i)(\forall i, j \leq n)$;

5: $\varphi(N_j, N_j) = |M(N_i, N_j)| = |\hat{E}^i| + |\hat{E}^j|$,·

6: If $\varphi(N_i, N_j) = 2m(m \in N^+)$ and $|\hat{E}^i| = |\hat{E}^j|$ Then the elements of N_i and N_j have similar order;

7: If $\varphi(N_j, N_j) = 2m + 1(m \in N^+)$, then $|\hat{E}^i| \neq |\hat{E}^j|$, that is, $|\hat{E}^i| < |\hat{E}^j|$ or $|\hat{E}^i| > |\hat{E}^j|$ and there is an order relation among the elements of N_j and N_i.

4. Performance Validation

This section inspects the face mask detection results of the WSDMDL-FMD technique on Kaggle dataset [26]. Table 1 reports detailed face and mask detection results obtained by the WSDMDL-FMD technique and existing DL models [27].

Table 1: Face and Mask detection outcome of WSDMDL-FMD approach with existing DL approaches

Model	Face Detection		Mask Detection	
	Precision	Recall	Precision	Recall
RetinaFaceMask-MobileNet	83.00	95.60	82.30	89.10
RetinaFaceMask-ResNet	91.90	96.30	93.40	94.50
DL-ARRCS-ResNet50	99.20	99.00	98.92	98.24
WSDMDL-FMD	99.57	99.37	99.24	98.81

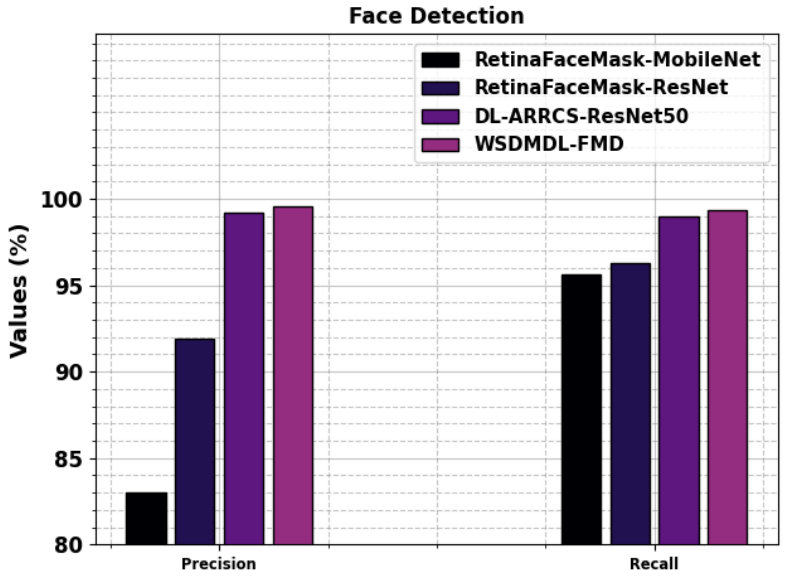

Figure 3: Face detection outcome of WSDMDL-FMD approach with existing DL approaches

In Fig. 3, the face detection results of the WSDMDL-FMD technique can be compared to other methods. The results portrayed the proficiency of the WSDMDL-FMD technique in face detection. In terms of $prec_n$, the WSDMDL-FMD technique demonstrates increased $prec_n$ of 99.57% whereas the RetinaFaceMask-MobileNet, RetinaFaceMask-ResNet, and DL-ARRCS-ResNet50 models attain decreased $prec_n$ of 83.00%, 91.90%, and 99.20%, correspondingly. Also, in terms of $reca_l$, the WSDMDL-FMD method validates better $reca_l$ of 99.37%

DOI: https://doi.org/10.54216/IJNS.250116
Received: April 12, 2024 Revised: May 02, 2024 Accepted: June 17, 2024

while the RetinaFaceMask-MobileNet, RetinaFaceMask-ResNet, and DL-ARRCS-ResNet50 methods accomplish decreased $reca_l$ of 95.60%, 96.30%, and 99.00%, correspondingly.

In Fig. 4, the mask detection outcomes of the WSDMDL-FMD method are compared to other methods. The outcomes depicted the ability of the WSDMDL-FMD method on mask recognition. In terms of $prec_n$, the WSDMDL-FMD method reveals improved $prec_n$ of 99.24% while the RetinaFaceMask-MobileNet, RetinaFaceMask-ResNet, and DL-ARRCS-ResNet50 techniques accomplish reduced $prec_n$ of 82.30%, 93.40%, and 98.92%, correspondingly. Also, in terms of $reca_l$, the WSDMDL-FMD system determines improved $reca_l$ of 98.81% while the RetinaFaceMask-MobileNet, RetinaFaceMask-ResNet, and DL-ARRCS-ResNet50 methods accomplish reduced $reca_l$ of 89.10%, 94.50%, and 98.24%, correspondingly.

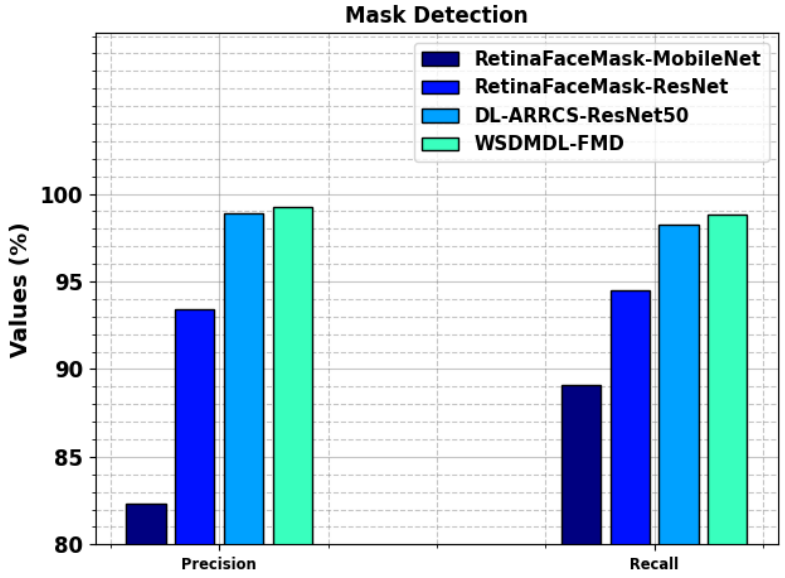

Figure 4: Mask detection outcome of WSDMDL-FMD approach with existing DL approaches

In Fig. 5, the training and validation accuracy outcomes of the WSDMDL-FMD method under Face detection are established. The accuracy values are calculated for 0-25 epochs. The figure emphasized that the training and validation accuracy values display a growing inclination which reported the capability of the WSDMDL-FMD method with enriched performance over numerous iterations.

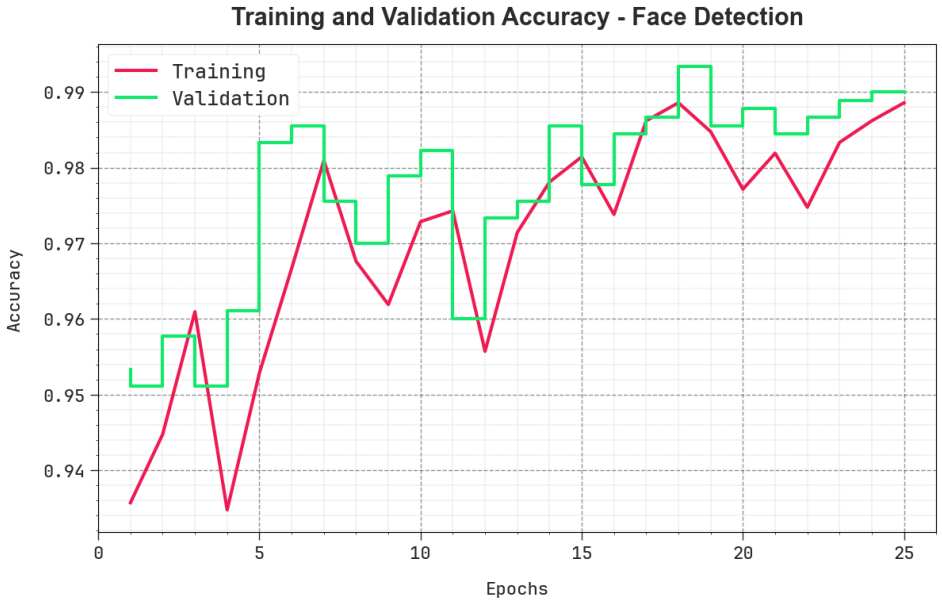

Figure 5: $Accu_y$ curve of WSDMDL-FMD approach under Face detection

DOI: https://doi.org/10.54216/IJNS.250116
Received: April 12, 2024 Revised: May 02, 2024 Accepted: June 17, 2024

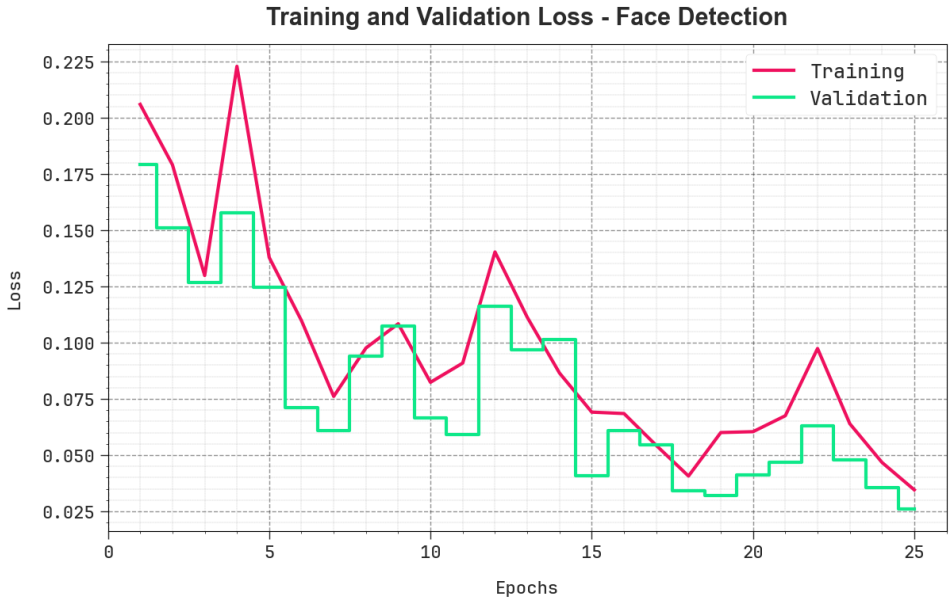

Figure 6: Loss curve of WSDMDL-FMD approach under Face detection

In Fig. 6, the training and validation loss graph of the WSDMDL-FMD method under Face detection is exhibited. The loss values are calculated for 0-25 epochs. It is characterized that the training and validation accuracy values demonstrate a declining inclination, reporting the ability of the WSDMDL-FMD method to balance a tradeoff between data fitting and generalization.

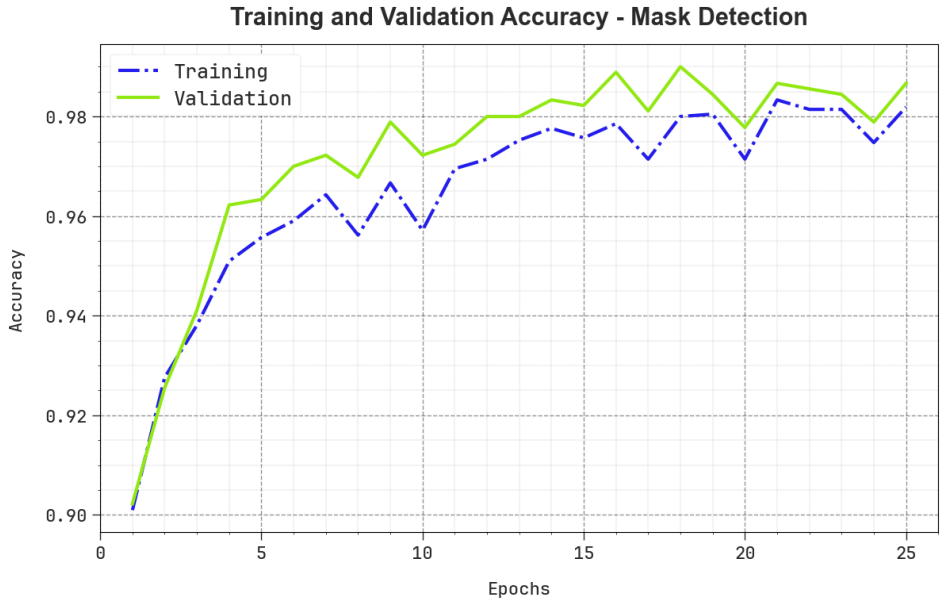

Figure 7: $Accu_y$ curve of WSDMDL-FMD approach under Mask detection

DOI: https://doi.org/10.54216/IJNS.250116
Received: April 12, 2024 Revised: May 02, 2024 Accepted: June 17, 2024

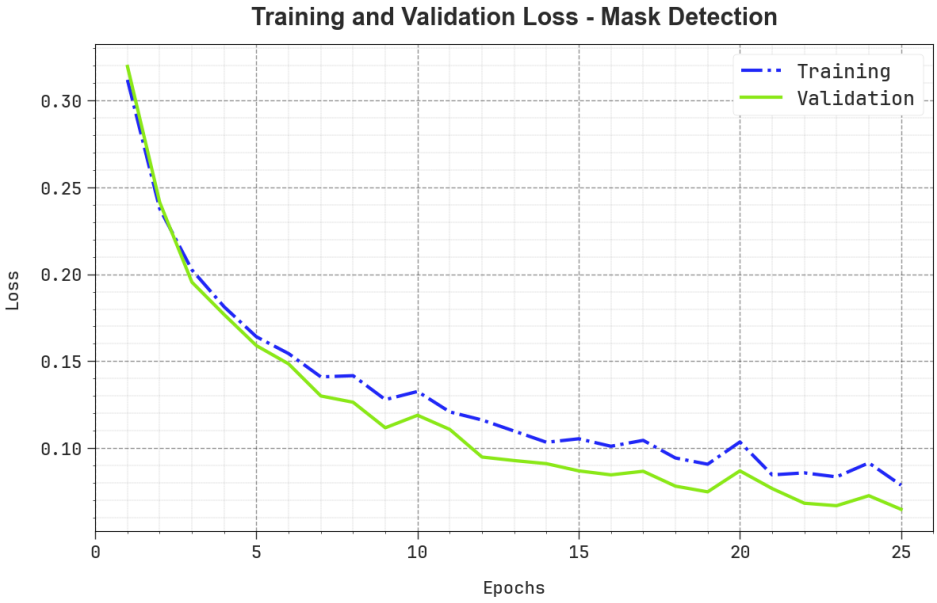

Figure 8: Loss curve of WSDMDL-FMD approach under Mask detection

In Fig. 7, the training and validation accuracy results of the WSDMDL-FMD method under Mask detection are validated. The accuracy values are calculated for 0-25 epochs. The figure emphasized that the training and validation accuracy values display a growing tendency which reported the capability of the WSDMDL-FMD method with enriched performance over several iterations.

In Fig. 8, the training and validation loss graph of the WSDMDL-FMD method under Mask detection is demonstrated. The loss values are calculated for 0-25 epochs. It is characterized that the training and validation accuracy values demonstrate a declining tendency, reporting the ability of the WSDMDL-FMD method to balance a tradeoff between data fitting and generalization.

Thus, the results guaranteed that the WSDMDL-FMD technique proficiently detects the face masks.

5. Conclusion

In this manuscript, we offer the design of WSDMDL-FMD technique for smart city environment. The WSDMDL-FMD technique proficiently discriminates the facial images with the presence or absence of masks. The WSDMDL-FMD technique comprises two stages: Mask RCNN-based face detection and WSDM-based face mask classification. Primarily, the WSDMDL-FMD technique uses Mask RCNN-based face detection. Next, the CNN model derives features from the detected faces and its hyperparameters can be chosen by COA. For face mask classification, the WSDMDL-FMD technique applies WSDM model. To evaluate the results of the WSDMDL-FMD technique, a series of experiments were involved. The obtained outcomes stated that the WSDMDL-FMD method reaches superior performance than other approaches

Funding: "This research received no external funding"

Conflicts of Interest: "The authors declare no conflict of interest."

References

[1] Smarandache, F., Neutrosophic set a generalization of the intuitionistic fuzzy sets. Inter. J. Pure Appl. Math., 24, 287 – 297, 2005.
[2] Mathew, L.P., Sebastian, L. and Thankachan, B., 2024. Some Operations on Trapezoidal Single Valued Neutrosophic Fuzzy Numbers. International Journal of Neutrosophic Science, 23(3), pp.29-9.
[3] Noaman, I.A.R., Hasan, A.H. and Ahmed, S.M., 2024. Optimizing Weibull Distribution Parameters for Improved Earthquake Modeling in Japan: A Comparative Approach. International Journal of Neutrosophic Science, 24(1), pp.65-5.
[4] Doaa Nihad Tomma, L. A. A. Al-Swidi. "Necessary and Sufficient Conditions for a Stability of the Concepts of Stable Interior and Stable Exterior via Neutrosophic Crisp Sets." International Journal of Neutrosophic Science, Vol. 24, No. 1, 2024 ,PP. 87-93

DOI: https://doi.org/10.54216/IJNS.250116
Received: April 12, 2024 Revised: May 02, 2024 Accepted: June 17, 2024

[5] Mathews, P., Sebastian, L. and Thankachan, B., 2024. Neutrosophic Fuzzy Score Matrices: A Robust Framework for Advancing Medical Diagnostics. International Journal of Neutrosophic Science, 23(3), pp.08-8.
[6] R. Saarumathi, W. Ritha. (2024). A Legitimate Productive Repertoire Replica Betwixt Envirotech Outlay Towards Fragile Commodities Using Trapezoidal Neutrosophic Fuzzy Number. International Journal of Neutrosophic Science, 24 (1), 104-118.
[7] G.J. Chowdary, N.S. Punn, S.K. Sonbhadra, S. Agarwal, Face Mask Detection using Transfer Learning of InceptionV3, in: International Conference on Big Data Analytics, Springer, Cham, 2020, pp. 81-90, pp. 1–11.
[8] S. Yang, P. Luo, C.C. Loy, X. Tang, WIDER FACE: A face detection benchmark, in: Proceedings of the IEEE Computer Society Conference on Computer Vision and Pattern Recognition, 2016.
[9] B. Yang, J. Yan, Z. Lei, S.Z. Li, Fine-grained evaluation on face detection in the wild, in: 2015 11th IEEE International Conference and Workshops on Automatic Face and Gesture Recognition, FG 2015, 2015.
[10] V. Jain, E. Learned-Miller, Fddb: A benchmark for face detection in unconstrained settings, UMass Amherst Tech. Rep., 2010, vol. 2, no. 4, UMass Amherst technical report, 2010.
[11] M. Inamdar, N. Mehendale, Real-Time Face Mask Identification Using Facemasknet Deep Learning Network, SSRN Electron. J. (2020).
[12] Habib, S., Alsanea, M., Aloraini, M., Al-Rawashdeh, H.S., Islam, M. and Khan, S., 2022. An efficient and effective deep learning-based model for real-time face mask detection. Sensors, 22(7), p.2602.
[13] Alsaheel, A., Alhassoun, R., Alrashed, R., Almatrafi, N., Almallouhi, N. and Albahli, S., 2023. Deep Fakes in Healthcare: How Deep Learning Can Help to Detect Forgeries. Computers, Materials & Continua, 76(2).
[14] Albahli, S. and Nawaz, M., 2023. MedNet: Medical deepfakes detection using an improved deep learning approach. Multimedia Tools and Applications, pp.1-19.
[15] Alajlan, N.N. and Ibrahim, D.M., 2022. TinyML: Enabling of inference deep learning models on ultra-low-power IoT edge devices for AI applications. Micromachines, 13(6), p.851.
[16] Alhasson, H.F., Almozainy, E., Alharbi, M., Almansour, N., Alharbi, S.S. and Khan, R.U., 2023. A Deep Learning-Based Mobile Application for Monkeypox Detection. Applied Sciences, 13(23), p.12589.
[17] Mostafa, S.A., Ravi, S., Zebari, D.A., Zebari, N.A., Mohammed, M.A., Nedoma, J., Martinek, R., Deveci, M. and Ding, W., 2024. A YOLO-based deep learning model for Real-Time face mask detection via drone surveillance in public spaces. Information Sciences, p.120865.
[18] Naseri, R.A.S., Kurnaz, A. and Farhan, H.M., 2023. Optimized face detector-based intelligent face mask detection model in IoT using deep learning approach. Applied Soft Computing, 134, p.109933.
[19] Sheikh, B.U.H. and Zafar, A., 2024. Untargeted white-box adversarial attack to break into deep learning based COVID-19 monitoring face mask detection system. Multimedia Tools and Applications, 83(8), pp.23873-23899.
[20] AL-Ghamdi, A.S., Alshammari, S.M. and Ragab, M., 2023. Deep Learning Based Face Mask Detection in Religious Mass Gathering During COVID-19 Pandemic. Computer Systems Science & Engineering, 46(2).
[21] Yasaswi, B., 2024. AOA based masked region-CNN model for detection of parking space in IoT environment. International Research Journal of Multidisciplinary Technovation, 6(1), pp.97-108.
[22] Vu, V.Q., Tran, M.Q., Amer, M., Khatiwada, M., Ghoneim, S.S. and Elsisi, M., 2023. A practical hybrid IoT architecture with deep learning technique for healthcare and security applications. Information, 14(7), p.379.
[23] Fontana, G., Calabrese, M., Agnusdei, L., Papadia, G. and Del Prete, A., 2024. SolDef_AI: An Open Source PCB Dataset for Mask R-CNN Defect Detection in Soldering Processes of Electronic Components. Journal of Manufacturing and Materials Processing, 8(3), p.117.
[24] Zahra, U., Khan, M.A., Alhaisoni, M., Alasiry, A., Marzougui, M. and Masood, A., 2023. An Integrated Framework of Two-Stream Deep Learning Models Optimal Information Fusion for Fruits Disease Recognition. IEEE Journal of Selected Topics in Applied Earth Observations and Remote Sensing.
[25] Gör, H., 2024. Feasibility of Six Metaheuristic Solutions for Estimating Induction Motor Reactance. Mathematics, 12(3), p.483.
[26] Khan, M.J., Kumam, P., Liu, P., Kumam, W. and Ashraf, S., 2019. A novel approach to generalized intuitionistic fuzzy soft sets and its application in decision support system. Mathematics, 7(8), p.742.
[27] https://www.kaggle.com/datasets/mrviswamitrakaushik/facedatahybrid
[28] Sethi, S., Kathuria, M. and Kaushik, T., 2021. Face mask detection using deep learning: An approach to reduce risk of Coronavirus spread. Journal of biomedical informatics, 120, p.103848.

DOI: https://doi.org/10.54216/IJNS.250116
Received: April 12, 2024 Revised: May 02, 2024 Accepted: June 17, 2024